Research Article

MOLECULAR PAIN

Molecular Pain
Volume 13: 1–10

DOI: 10.1177/1744806917737461
journals.sagepub.com/home/mpx

SAGE

Abnormal functional integration across core brain networks in migraine without aura

Dahua Yu[1,*], Kai Yuan[1,2,*], Lin Luo[3], Jinquan Zhai[3], Yanzhi Bi[2], Ting Xue[1], Xiaoying Ren[1], Ming Zhang[1], Guoyin Ren[1] and Xiaoqi Lu[1]

Abstract

Background: As a complex subjective experience, pain processing may be related to functional integration among intrinsic connectivity networks of migraine patients without aura. However, few study focused on the pattern alterations in the intrinsic connectivity networks of migraine patients without aura.

Results: Thirty-one migraine patients without aura and 31 age- and education-matched healthy controls participated in this study. After identifying the default mode network, central executive network and salience network as core intrinsic connectivity networks by using independent component analysis, functional connectivity, and effective connectivity during the resting state were used to investigate the abnormalities in intrinsic connectivity network interactions. Migraine patients without aura showed decreased functional connectivity among intrinsic connectivity networks compared with healthy controls. The strength of causal influences from the right frontoinsular cortex to the right anterior cingulate cortex became weaker, and the right frontoinsular cortex to the right medial prefrontal cortex became stronger in migraine patients without aura.

Conclusions: These changes suggested that the salience network may play a major role in the pathophysiological features of migraine patients without aura and helped us to synthesize previous findings into an aberrant network dynamical framework.

Keywords

Intrinsic connectivity networks, independent component analysis, functional connectivity, Granger causality analyses

Date received: 20 February 2017; revised: 19 August 2017; accepted: 21 September 2017

Background

As a common type of primary headache syndromes, migraine was associated with repeated pain attacks, which may result in deficits of central pain processing.[1,2] With the help of neuroimaging technology, structural and functional abnormalities in several brain regions were reported in migraine patients.[1–6] As a complex subjective experience, pain processing in migraine patients may be related to functional integration among intrinsic connectivity networks (ICNs).[5,7,8]

Previous studies demonstrated that correlated spontaneous fluctuations occur within several spatially distinct and functionally related groups of brain regions consisting of the human brain's ICNs during the resting state.[9] As data-driven analytical method, independent component analysis (ICA) was used to explore these ICNs during the resting state.[10] The most important

[1]Inner Mongolia Key Laboratory of Pattern Recognition and Intelligent Image Processing, School of Information Engineering, Inner Mongolia University of Science and Technology, Baotou, Inner Mongolia, China
[2]Life Sciences Research Center, School of Life Science and Technology, Xidian University, Xi'an, Shaanxi, China
[3]Department of Medical Imaging, The First Affiliated Hospital of Baotou Medical College, Inner Mongolia University of Science and Technology, Baotou, Inner Mongolia, China

*Dahua Yu and Kai Yuan contributed equally to this article.

Corresponding authors:
Kai Yuan, School of Life Science and Technology, Xidian University, Xi'an 710071, China.
Email: kyuan@xidian.edu.cn
Xiaoqi Lu, Inner Mongolia Key Laboratory of Pattern Recognition and Intelligent Image Processing, School of Information Engineering, Inner Mongolia University of Science and Technology, Baotou, Inner Mongolia 014010, China.
Email: lxiaoqi@imust.cn

networks of these stable ICNs were demonstrated as core ICNs, including (1) the default mode network (DMN), which includes the ventromedial prefrontal cortex and posterior cingulate cortex (PCC); (2) the central executive network (CEN), which includes the dorsolateral prefrontal cortex (DLPFC) and posterior parietal cortex (PPC); and (3) the salience network (SN), which includes the anterior cingulate cortex (ACC) and the frontoinsular cortex (FIC).[9] The ICNs expressed close correspondence during the resting state or task-related state, which was associated with cognition, emotion, and pain systematically.[9] It is noteworthy that the right FIC (rFIC) as the key node of SN was revealed to act as the critical and causal hub coordinating with the CEN and the DMN.[11–15] Consistent with this view, several studies investigated the role of ICNs in migraine patients.[16–18] The structural and functional abnormalities in the ACC and insula may reveal the abnormalities in the SN.[1,2,16,17,19–23] In addition, the abnormalities in the prefrontal cortex (PFC) and PCC as parts of CEN and DMN were also reported.[1,2,16–23] In our previous study, we used ICA with dual-regression technique to identify the voxel-wise group differences of three core ICNs. Compared with the healthy controls, migraine patients without aura (MwoA) showed aberrant intrinsic connectivity within the bilateral CEN and SN and increased connectivity between the DMN and right CEN to the insula.[16] The whole brain voxel-wise contrast results were related to the brain regions with different "connectivity" to each ICN in MwoA. Despite the prominent advantages of whole brain voxel-wise contrast method of ICA, it might provide less features of functional interaction of core ICNs simultaneously.[10] However, few studies focused on the pattern alteration of functional integration between the ICNs in MwoA.

Therefore, in the present study, we investigated functional abnormalities within and between the DMN, CEN, and SN in MwoA by using ICA, functional connectivity (FC), and Granger causality analyses (GCA). Due to the critical role of the SN among these ICNs, we hypothesized that the SN might show a critical role in FC pattern in MwoA. The interactions among ICNs may improve our understanding of migraine pathology from a system neuroscience perspective.

Methods

Subjects

This study was approved by the Medical Ethics Committee of the First Affiliated Hospital of Baotou Medical College, Inner Mongolia University of Science and Technology, Baotou, China. All participants signed the informed consent after the experimental procedure was fully explained. All MwoA were screened following the International Headache Society criteria.[24] Then, age- and gender-matched healthy controls were enrolled, which neither did not have any sort of headache nor had family members who suffered headache. Inclusion criteria for both groups were no physical illness as assessed according to clinical evaluations and medical records, no pregnancy or menstrual period in female subjects, no addiction or drug abuse, no neurological disease or claustrophobia, and no other type of pain. All of the participants were measured by the Edinburgh Handedness Inventory as right-handed.[25]

All subjects underwent urine drug screening to exclude the possibility of substance abuse before the scan. Patients were having a migraine attack neither at least 72 h prior to scanning[26] nor on the day following the scan. At last, 31 MwoA (22 females, aged 22–57 years, mean age, 36.2 ± 10.2 years) and 31 age- and gender-matched healthy controls (22 females, aged 24–55 years, mean age, 36.5 ± 13.1 years) were recruited in our study. Average pain intensity of migraine patients was rated as 5.2 ± 1.7 on a 0–10 visual analog scale from attacks in the past four weeks, with 0 being no pain and 10 being the most intense pain imaginable. Attack frequency in the past four weeks was also rated. The clinical and demographic characteristics of participants are shown in Table 1.

Data acquisition

All image data were acquired on a 3T Philips scanner (Achieva; Philips Medical Systems, Best, The Netherlands) at the First Affiliated Hospital of Baotou Medical College, Inner Mongolia University of Science and Technology, Baotou, China. The heads of the subjects were restrained with foam pads and positioned carefully with comfortable support. To reduce scanner noise,

Table 1. Clinical details of migraine patients without aura and healthy controls (mean ± SD).

Clinical details	Migraine patients without aura ($n = 31$)	Healthy controls ($n = 31$)
Age (years)	36.2 ± 10.2	36.5 ± 13.1
Sex (F, female; M, male)	22 F, 9 M	22 F, 9 M
Disease duration (years)	10.4 ± 7.0	—
Information of migraine attacks during past 4 weeks		
Attack frequency (times)	5.5 ± 3.9	—
Average pain intensity (0–10)[a]	5.2 ± 1.7	—

Data are means ± standard deviations.
[a]Average pain intensity by visual analog scale (VAS) on a 0–10 scale based on the attacks in the past 4 weeks, with 0 being no pain and 10 being the most intense pain imaginable.

earplugs were used during the scan. Prior to the resting state functional magnetic resonance imaging (fMRI) run for each subject, a high-resolution T1 structural image was acquired using a magnetization prepared rapid acquisition gradient echo pulse sequence with a voxel size of 1 mm^3 (repetition time (TR) = 8.4 ms; echo time (TE) = 3.8 ms; data matrix = 240 × 240; axial slices = 176; field of view (FOV) = 240 × 240 mm^2). Then, the resting state functional images were obtained with an echo-planar imaging sequence (30 contiguous axial slices with slice thickness = 5 mm, TR = 2,000 ms, TE = 30 ms, flip angle = 90°, FOV = 224 × 224 mm^2, data matrix = 64 × 64, and total volumes = 180). Acquisition order of functional images was interleaved. Subjects were instructed to stay awake and keep their eyes closed, not to think about anything during the entire 6-min functional scan. After the scan, all the participants were asked whether they remained awake during the whole procedure. Two expert radiologists examined the images of all participants to exclude any clinically silent lesions.

Data analysis

The image data during the resting state was preprocessed following the standard data preprocessing strategy as part of the 1000 Functional Connectomes Project (http://www.nitrc.org/projects/fcon_1000),[27] using FMRIB's Software Library (FSL) v5.0.0 (http://www.fmrib.ox.ac.uk/fsl/) and Automated Functional Neuro-Imaging (AFNI, http://afni.nimh.nih.gov/afni) software. Data preprocessing includes (1) discarding the first five volumes to eliminate nonequilibrium effects of magnetization and allow subjects to get used to the scanning environment; (2) slice timing correction; (3) rigid-body head motion correction (3 displacements and 3 rotations); (4) obliquity transform to the structural image; (5) affine coregistration to the skull-stripped structural image; (6) standard spatial transform to the MNI152 template; (7) spatial smoothing (6 mm full width at half maximum); and (8) intensity normalization to a whole-brain median of 1000. Nuisance regression and bandpass filtering (0.01–0.1 Hz) alone are often insufficient to control head movement-induced noise. Therefore, denoising steps included: (9) time series despiking (wavelet domain); (10) nuisance signal regression including the six motion parameters, their first-order temporal derivatives, and ventricular cerebrospinal fluid signal (13-parameter regression); and (11) a temporal Fourier filter.

ICA processing. The ICA approach[28] was applied to investigate the ICNs in MwoA and healthy controls in the current study. The preprocessed functional images of all subjects were temporally concatenated to create a single four-dimensional data set for the following analysis. ICA was processed by Multivariate Exploratory Linear Decomposition into Independent Components ICA v3.1 as a part of FSL. The number of independent components was limited as 25 to avoid independent components splitting into subcomponents. The ICNs of interest, including the DMN, bilateral CEN and SN, were selected from these components as the "best-fit" network component described in previous studies.[14,16]

Region of interest selection. The key nodes of ICNs were defined based on the peaks of the ICA clusters. The highest z-scores within each cluster in the bilateral FIC and ACC on the SN ICA map (Figure 1, the first row), in the bilateral MPFC and PCC on the DMN ICA map (Figure 1, the second row), and in the bilateral DLPFC and PPC on the bilateral CEN ICA map (Figure 1, the third and fourth rows) were selected as seed points (shown in Table 2). The regions of interest (ROIs) of bilateral cerebral hemispheres were constructed by drawing a sphere of 5 mm radius with the seed point as centers. The ROI selection method was widely used in functional and effective connectivity studies.[14,29–31]

Functional connectivity analysis. The resting-state time series in each ROI were extracted and averaged. Then, partial correlation was used as the measure of FC between each two of the unilateral ROIs, controlling for the effect of other regions. In consideration of our analysis investigated FC in three ICNs, the partial correlation approach may provide significant advantages over the pure correlation approach.[32] A Fisher's r-to-z transform was applied to account for the nonnormality of partial correlations.

Multivariate GCA. By using REST-GCA as a part of the Resting-State fMRI Data Analysis Toolkit (REST, by Song Xiao-Wei et al., http://www.restfmri.net), ROI-wised multivariate coefficients' GCA were evaluated among hemisphere ICNs. If the signed-path coefficient is significantly larger or smaller than zero, a time series can be defined as a significant Granger cause to another time series. As the signed-path coefficients are considered to fit normal distribution, t test was used for group-level inference.[33]

One-sample t test and two-sample t test (both $p < 0.05$) with bootstrap resampling (1000 iterations) were analyzed for both functional and effective connectivity by using PASW Statistics Version 18.0 (Formerly SPSS Statistics, SPSS Inc., Chicago, IL). The bootstrap resampling is a method for deriving robust estimates of standard errors, confidence intervals, and hypothesis tests, which may be an appropriate way to control and check the stability of the results.

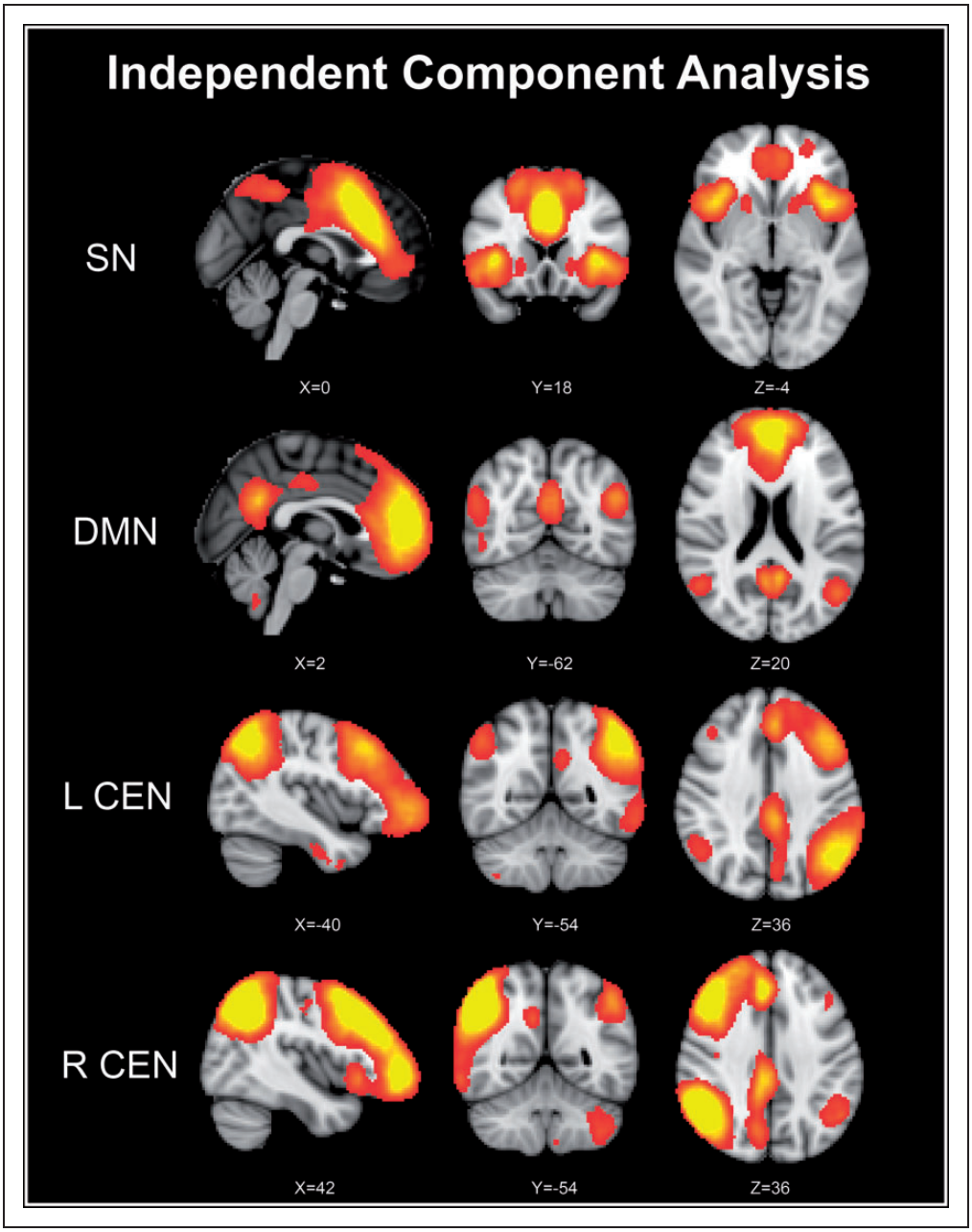

Figure 1. Identifying key nodes of ICNs using ICA. DMN: default mode network; ICA: independent component analysis; ICNs: intrinsic connectivity networks; L CEN: left central executive network; R CEN: right central executive network; SN: salience network.

At last, a series of Pearson's correlation analyses were performed to examine the significant correlation ($p < 0.05$) of the functional and effective connectivity to pain intensity, attack frequency, and duration of migraine.

Results

Comparison of FC

Partial correlations between pairs of ROIs in each hemisphere were calculated. FC results within MwoA and healthy controls are shown in the first and second rows of Figure 2. The key nodes within ICNs exhibited significant higher FC in both hemispheres as green edge in DMN, blue edge in CEN, and red edge in SN. Compared with healthy controls, MwoA showed decreased FC between right ACC and PFC (for bootstrap resampling, $p = 0.038$) and between right ACC and PCC (for bootstrap resampling, $p = 0.012$). In detail, FC values between right ACC and PFC were 0.375 ± 0.201 (mean $\pm$ standard deviation) in healthy controls and 0.259 ± 0.214 in MwoA. FC values between right ACC

Table 2. Coordinates of SN, CEN, and DMN regions derived from ICA of resting state data.

Network	Region	Peak MNI coordinates (mm)	z scores
Right DMN	rMPFC	5, 60, 12	11.0072
	rPCC	5, −54, 26	8.26187
Right CEN	rDLPFC	44, 20, 42	14.7049
	rPPC	48, −54, 48	21.7601
Right SN	rFIC	38, 16, 2	10.5872
	rACC	5, 25, 26	13.0995
Left DMN	lMPFC	−5, 60, 12	11.2533
	lPCC	−7, −54, 26	9.40507
Left CEN	lDLPFC	−40, 22, 40	9.15522
	lPPC	−44, −62, 50	12.8235
Left SN	lFIC	−38, 16, 2	10.2338
	lACC	−5, 25, 26	12.4242

ACC: anterior cingulate cortex; CEN: central executive network; DLPFC: dorsolateral prefrontal cortex; DMN: default mode network; FIC: frontoinsular cortex; ICA: independent component analysis; l: left; MNI: Montreal Neurological Institute; MPFC: medial prefrontal cortex; PCC: posterior cingulate cortex; PPC: posterior parietal cortex; r: right; SN: salience network.

and PCC were -0.122 ± 0.177 in healthy controls and -0.003 ± 0.166 in MwoA. And in left hemisphere, MwoA showed decreased FC of the left insula–PFC (for bootstrap resampling $p = 0.037$) and the left PFC–PPC (for bootstrap resampling $p = 0.047$). In detail, FC values of the left insula–PFC were -0.223 ± 0.197 in healthy controls and -0.125 ± 0.179 in MwoA. FC values of the left PFC–PPC were -0.280 ± 0.234 in healthy controls and -0.160 ± 0.227 in MwoA. No increased FC was found MwoA.

Comparison of effective connectivity

Multivariate GCA was used to investigate causal interactions among the six network nodes in each hemisphere. Consistent with previous studies,[11,14] the rFIC showed significant direct causal influences to the right ACC, DLPFC, MPFC, and PCC (the first row of Figure 3). In MwoA, the rFIC similarly showed significant direct causal influences to the right ACC and the MPFC (the second row of Figure 3). Group differences analysis revealed that the strength of causal influences from the rFIC to the right ACC was significantly decreased (for bootstrap resampling $p = 0.040$) in MwoA compared with healthy controls, and the strength of causal influences from the rFIC to the right DLPFC was significantly increased (for bootstrap resampling $p = 0.012$; the third row of Figure 3). In detail, the strength of causal influences from the rFIC to the right ACC was 0.141 ± 0.163 in healthy controls and 0.068 ± 0.125 in MwoA. The strength of causal influences from the rFIC to the right DLPFC was -0.080 ± 0.129 in healthy controls and -0.002 ± 0.113 in MwoA. In the left hemisphere, only the strength of causal influences from the left PFC to the left PPC was significantly increased (for bootstrap resampling $p = 0.049$) in MwoA compared with healthy controls. In detail, the strength of causal influences from the left PFC to the left PPC was -0.088 ± 0.138 in healthy controls and -0.019 ± 0.125 in MwoA. The left FIC is not as the rFIC as a driver of network dynamics in accordance with a previous study.[11]

Correlation analysis

Correlation analysis results demonstrated that there were significant negative correlations between the FC values of the right ACC–PCC and average pain intensity in MwoA ($r = -0.4617$, $p = 0.0089$; Figure 4(a)). Moreover, the negative correlations were also found in MwoA between the decreased strength of causal influences from the rFIC to the right ACC and duration of migraine ($r = -0.3876$, $p = 0.0312$; Figure 4(b)) and between the increased strength of causal influences from the rFIC to the right DLPFC and attack frequency ($r = -0.3701$, $p = 0.0404$; Figure 4(c)).

Discussion

Frequent migraine attacks may be associated with functional abnormalities in several brain regions, which were mainly involved in pain processing.[1,2,4,34] As the SN impacts the DMN and CEN, efficient pain regulation may rely on the cooperation between core brain networks.[12–14,35] In the present study, we combined functional and effective connectivity to test functional changes within and between core ICNs. Compared with healthy controls, MwoA showed decreased FC of the right ACC–PFC, the right ACC–PCC, the left insula–PFC, and the left PFC–PPC (Figure 2). Similar to previous studies, the rFIC was identified as a causal outflow hub.[11,12,14] The strength of causal influences from the rFIC to the right ACC became weaker, and to the right DLPFC became stronger in MwoA (Figure 3). In addition, correlation analysis results revealed that the FC of the right ACC–PCC, the strength of causal influences from the rFIC to the right ACC and from the rFIC to the right DLPFC were correlated with clinical parameters in MwoA.

In the present study, decreased FC was shown between the right ACC and the PFC as well as the PCC in MwoA compared with healthy controls. Previous studies provided converging evidence that the FIC and ACC, as the key nodes of the SN, responded to the degree of subjective salience and was related with detecting, integrating, and filtering relevant

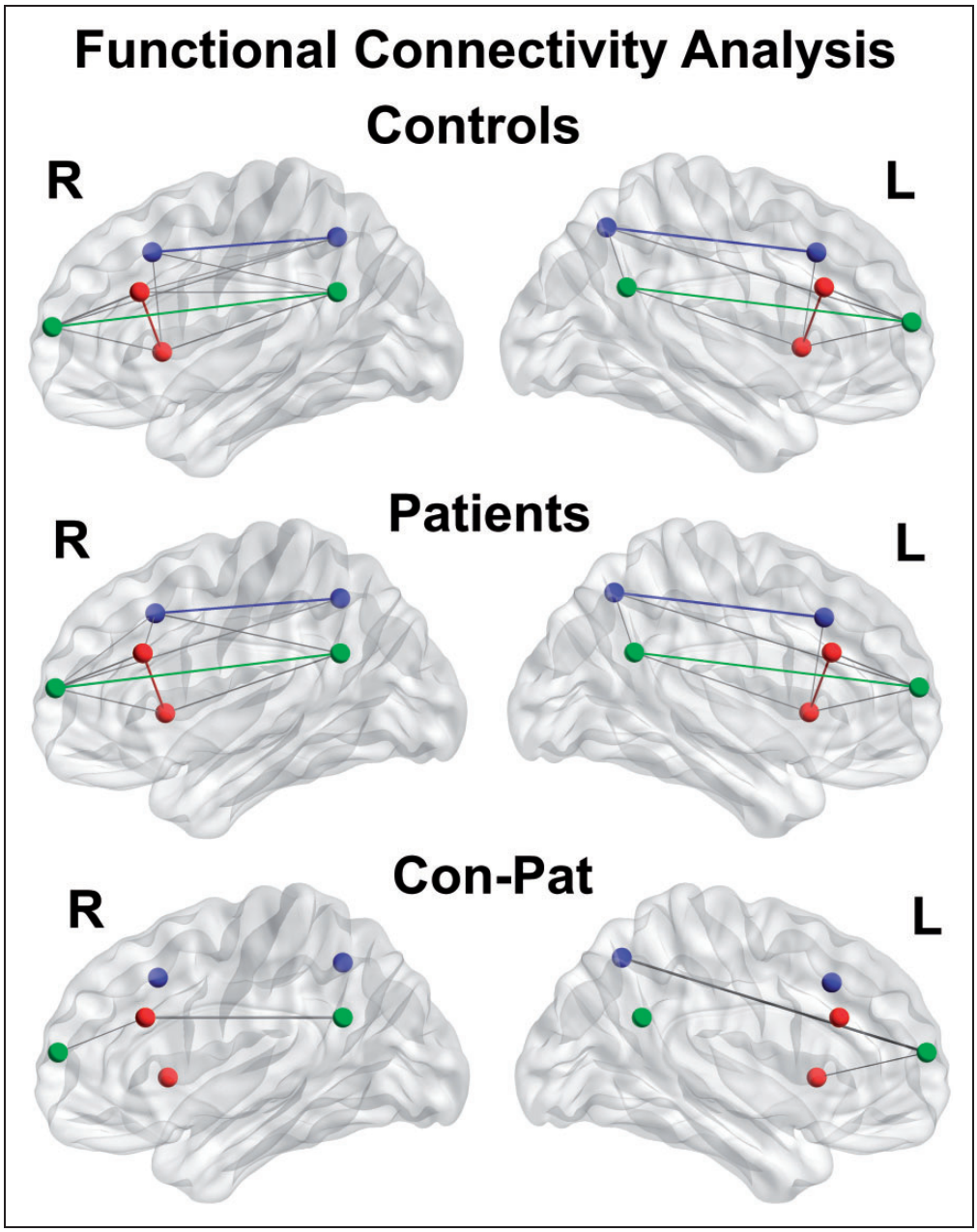

Figure 2. Functional connectivity measured by partial correlation, between the six key nodes of the SN (red), CEN (blue), and DMN (green). CEN: central executive network; DMN: default mode network; SN: salience network.

interoceptive, autonomic, and emotional information.[11,35] In task condition, the SN may initiate control signals that activate the CEN and deactivate the DMN.[11] In particular, the rFIC played a critical role with higher causal outflow in the interoceptive awareness of stimulus information processing in homeostatic states, such as pain, empathy, and disgust.[35] Moreover, the FIC and the ACC were commonly reported in structural[4] and functional studies[1,2,4,20,26,36] of migraine, which were mainly involved in pain-related processing.[4] The ACC was involved in the affective responses of pain and endogenous pain control.[4,16,20,21,34] The insula was discovered as a main area of pain integration and response to stimuli.[1,2,16,17,19–21] The SN is associated with both physical pain and empathy for pain, along with information integration about an impending stimulation to perceptual decision-making in the context of pain.[37] It is noteworthy that Aderjan et al.[36] used a 20-min trigeminal pain paradigm to stimulate both healthy controls and MwoA daily in three months. The fMRI result revealed that the ACC showed completely opposite behavior in MwoA compared with healthy controls,

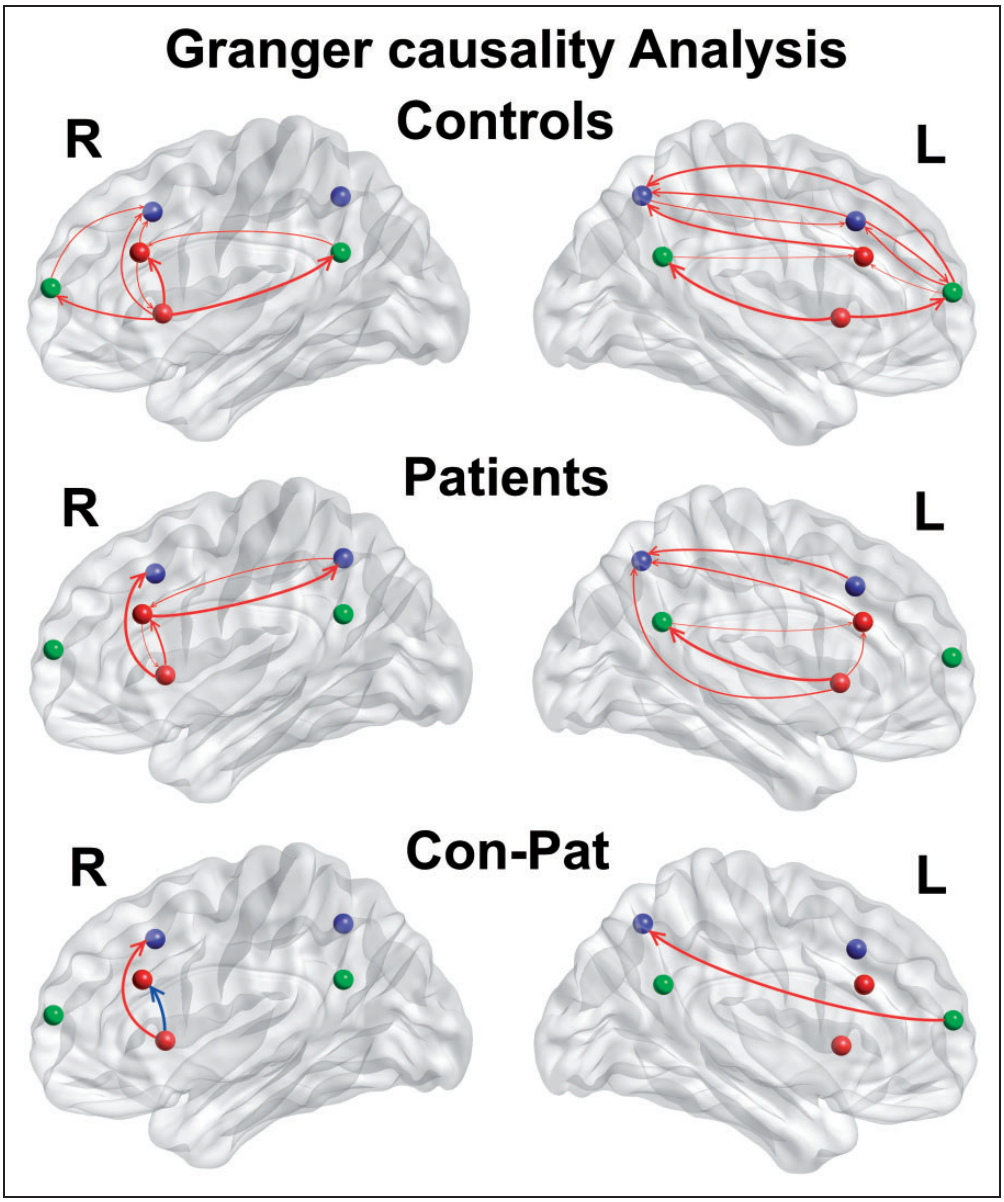

Figure 3. Effective connectivity measured by GCA, between the six key nodes of the SN (red), CEN (blue), and DMN (green). The red color of arrows in the third row means the increased strength of causal influences, and blue color means the decreased strength. CEN: central executive network; DMN: default mode network; SN: salience network; GCA: Granger causality analyses.

nevertheless, their behavioral pain ratings were not different. In more detail, the activation in the ACC increased in healthy control subjects, whereas it decreased in migraine patients.[36] The opposite behavior of the ACC during the long-term stimulation revealed the alteration of pain inhibitory circuits, which may be associated with the abnormal interaction from the rFIC to the ACC in the SN during the resting state. Present findings reveal that the dynamical framework of the SN, in particular the ACC, is dysfunctional in MwoA. Moreover, significant negative correlations were found between the FC of the right ACC–PCC and average pain intensity, which showed negatively higher ACC–PCC FC reported stronger average pain intensity. The FC of the right ACC–PCC was only significant in healthy controls (-0.122 ± 0.177) and not found in MwoA (-0.003 ± 0.166) (Figure 2). The negative correlations between FC and pain intensity were also reported in several previous migraine studies.[36,38,39] It may suggest that the FC of right ACC–PCC is associated with complex subjective experience of pain in MwoA.

On the other hand, the rFIC may enable to initiate control signals in task-related information processing to engage the ACC and the CEN.[11,35] Previous studies

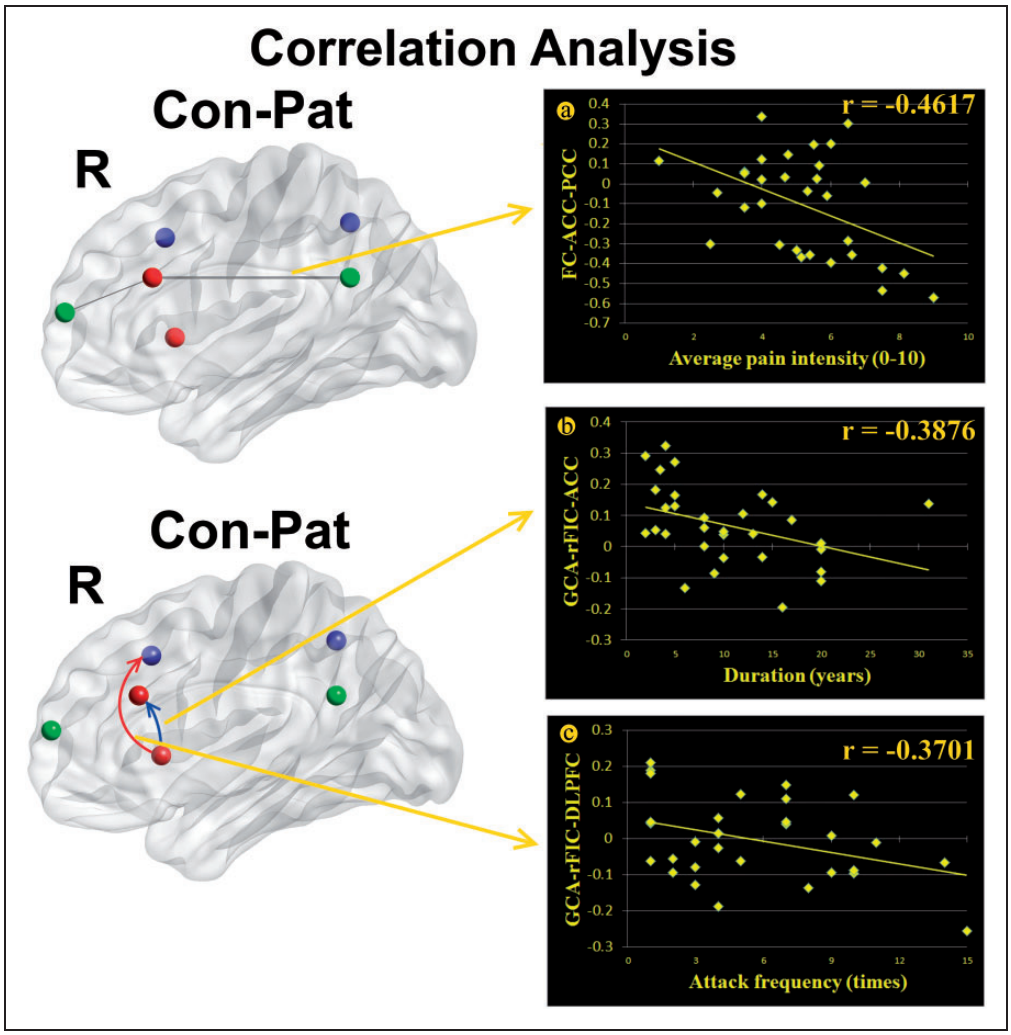

Figure 4. Correlation analysis results demonstrated that there were significant negative correlation between the functional connectivity between right ACC–PCC and average pain intensity in MwoA ($r = -0.4617$, $p = 0.0089$) (a). Moreover, the negative correlations were also found in MwoA between the decreased strength of causal influences from the rFIC to the right ACC and duration of migraine ($r = -0.3876$, $p = 0.0312$) (b), and between the increased strength of causal influences from the rFIC to the right DLPFC and attack frequency ($r = -0.3701$, $p = 0.0404$) (c).

revealed that if the ACC is dysfunctional, the FIC may trigger alternate control mechanisms via the CEN to maintain the balance of cognitive, homeostatic, and affective systems.[11,35] In our result, increased causal influences from the rFIC to the right DLPFC may be a kind of compensation to the dysfunctional ACC with decreased causal influence from the rFIC to the right ACC. It also may reveal that this compensation was involved with the normal pain ratings and less behavioral abnormality in MwoA.[36] Moreover, correlation analysis results demonstrated that there were significant negative correlation between the decreased strength of causal influences from the rFIC to the right ACC and duration of migraine. It may suggest that migraine has accumulated effects on the strength of causal influences from the rFIC to the right ACC. Significant negative correlations were also found between increased strength of causal influences from the rFIC to the right DLPFC and attack frequency, which may suggest that attack frequency influenced the strength of causal influences from the rFIC to the right DLPFC. Our results suggested that the changes of effective connectivity might be related with the characteristic of migraine, which may help to synthesize previous findings in MwoA into an aberrant network dynamical framework of ICNs.

Limitation

The study is limited in the cross-sectional design and not possible to infer causality of the relationships between migraine attack and aberrant interaction of the ICNs. The relationships might be bidirectional and related to

some latent variables. Further longitudinal studies would be required to improve the understanding of it. Another limitation was that functional and effective connectivity analysis were evaluated only in each hemisphere. To fully understand the changes of interactions among brain regions in MwoA, more complicated analysis of interhemispheric interactions in functional and effective connectivity should be studied further. As a data-driven method, GCA was widely applied to time series to detect causal inferences, especially to blood-oxygen level dependent signals of fMRI to investigate effective connectivity between brain areas, which may be a key challenge for neuroscience and shed light on how the brain works.[40–42] However, the application of GCA to fMRI data was particularly controversial, since Granger causal inferences might be easily confounded by interregional differences in the hemodynamic response function.[43] Although the limitation exists, our findings were, at least partially, acceptable for the relationship between the brain core networks interaction in MwoA.

Conclusions

In the current study, we investigated functional interaction of the ICNs in MwoA. The SN in MwoA showed abnormal functional and effective connectivity in it and with the DMN and the CEN. These changes may suggest the SN play a major role in the pathophysiological features of MwoA and help us to synthesize previous findings into an aberrant network dynamical framework. However, a more comprehensive experimental design is needed to investigate the accurate roles of the interaction among these ICNs. We hope that our findings might improve the understanding of migraine mechanisms and provide potential diagnostic information in migraine patients.

Authors' Contributions

DY and KY carried out the experiment and wrote the manuscript. LL and JZ participated in the design and carried out the experiment of this study. TX performed the statistical analysis of this study. XR and MZ participated in the data processing. GR participated in the design of this study. XL made substantial contributions to the design and coordination of this study. YB revised the manuscript. All authors read and approved the final manuscript. DY and KY contributed equally to this article.

Declaration of Conflicting Interests

The author(s) declared no potential conflicts of interest with respect to the research, authorship, and/or publication of this article.

Funding

The author(s) disclosed receipt of the following financial support for the research, authorship, and/or publication of this article: This paper is supported by the National Natural Science Foundation of China under Grant Nos. 81571751, 81571753, 81301281, 61771266, 81701780, 81401488, 61179019, 81401478, 81271644, 81271546, 81271549, 81470816, and 81471737, the Fundamental Research Funds for the Central Universities under the Grant Nos. JB151204 and JB121405, the program for Young Talents of Science and Technology in Universities of Inner Mongolia Autonomous Region NJYT-17-B11, the Natural Science Foundation of Inner Mongolia under Grant Nos. 2014BS0610 and 2017MS(LH)0814, the program of Science and Technology in Universities of Inner Mongolia Autonomous Region NJZY17262, the Innovation Fund Project of Inner Mongolia University of Science and Technology under Grant Nos. 2015QNGG03 and 2014QDL002, and General Financial Grant the China Postdoctoral Science Foundation under Grant No. 2014M552416.

References

1. Borsook D, Veggeberg R, Erpelding N, et al. The insula: a "hub of activity" in migraine. *Neuroscientist* 2016; 22: 632–652.
2. Ellerbrock I, Engel AK and May A. Microstructural and network abnormalities in headache. *Curr Opin Neurol* 2013; 26: 353–359.
3. May A. Morphing voxels: the hype around structural imaging of headache patients. *Brain* 2009; 132: 1419–1425.
4. Schwedt TJ and Dodick DW. Advanced neuroimaging of migraine. *Lancet Neurol* 2009; 8: 560–568.
5. Peyron R, Laurent B and Garcia-Larrea L. Functional imaging of brain responses to pain. A review and meta-analysis. *Neurophysiol Clin* 2000; 30: 263–288.
6. Tedeschi G, Russo A and Tessitore A. Relevance of functional neuroimaging studies for understanding migraine mechanisms. *Expert Rev Neurother* 2013; 13: 275–285.
7. Apkarian AV, Bushnell MC, Treede RD, et al. Human brain mechanisms of pain perception and regulation in health and disease. *Eur J Pain* 2005; 9: 463–484.
8. Tracey I and Mantyh PW. The cerebral signature for pain perception and its modulation. *Neuron* 2007; 55: 377–392.
9. Fox MD, Snyder AZ, Vincent JL, et al. Intrinsic fluctuations within cortical systems account for intertrial variability in human behavior. *Neuron* 2007; 56: 171–184.
10. Zang ZX, Yan CG, Dong ZY, et al. Granger causality analysis implementation on MATLAB: a graphic user interface toolkit for fMRI data processing. *J Neurosci Methods* 2012; 203: 418–426.
11. Sridharan D, Levitin DJ and Menon V. A critical role for the right fronto-insular cortex in switching between central-executive and default-mode networks. *Proc Natl Acad Sci USA* 2008; 105: 12569–12574.
12. Menon V and Uddin LQ. Saliency, switching, attention and control: a network model of insula function. *Brain Struct Funct* 2010; 214: 655–667.
13. Bonnelle V, Ham TE, Leech R, et al. Salience network integrity predicts default mode network function after

traumatic brain injury. *Proc Natl Acad Sci USA* 2012; 109: 4690–4695.
14. Uddin LQ, Supekar KS, Ryali S, et al. Dynamic reconfiguration of structural and functional connectivity across core neurocognitive brain networks with development. *J Neurosci* 2011; 31: 18578–18589.
15. Moran LV, Tagamets MA, Sampath H, et al. Disruption of anterior insula modulation of large-scale brain networks in schizophrenia. *Biol Psychiatry* 2013; 74: 467–474.
16. Xue T, Yuan K, Zhao L, et al. Intrinsic brain network abnormalities in migraines without aura revealed in resting-state fMRI. *PLoS One* 2012; 7: e52927.
17. Tso AR, Trujillo A, Guo CC, et al. The anterior insula shows heightened interictal intrinsic connectivity in migraine without aura. *Neurology* 2015; 84: 1043–1050.
18. Russo A, Tessitore A, Giordano A, et al. Executive resting-state network connectivity in migraine without aura. *Cephalalgia* 2012; 32: 1041–1048.
19. Yu D, Yuan K, Qin W, et al. Axonal loss of white matter in migraine without aura: a tract-based spatial statistics study. *Cephalalgia* 2012; 33: 34–42.
20. Yu D, Yuan K, Zhao L, et al. Regional homogeneity abnormalities in patients with interictal migraine without aura: a resting-state study. *NMR Biomed* 2012; 25: 806–812.
21. Yuan K, Zhao L, Cheng P, et al. Altered structure and resting-state functional connectivity of the basal ganglia in migraine patients without aura. *J Pain* 2013; 14: 836–844.
22. Yuan K, Qin W, Liu P, et al. Reduced fractional anisotropy of corpus callosum modulates inter-hemispheric resting state functional connectivity in migraine patients without aura. *PLoS One* 2012; 7: e45476.
23. Jin C, Yuan K, Zhao L, et al. Structural and functional abnormalities in migraine patients without aura. *NMR Biomed* 2013; 26: 58–64.
24. Headache Classification Subcommittee of the International Headache Society. The international classification of headache disorders, 2nd edition. *Cephalalgia* 2004; 24 Suppl 1: 9–160.
25. Oldfield RC. The assessment and analysis of handedness: the Edinburgh inventory. *Neuropsychologia* 1971; 9: 97–113.
26. Moulton E, Becerra L, Maleki N, et al. Painful heat reveals hyperexcitability of the temporal pole in interictal and ictal migraine states. *Cereb Cortex* 2011; 21: 435–448.
27. Biswal BB, Mennes M, Zuo X-N, et al. Toward discovery science of human brain function. *Proc Natl Acad Sci USA* 2010; 107: 4734–4739.
28. Beckmann CF and Smith SM. Probabilistic independent component analysis for functional magnetic resonance imaging. *IEEE Trans Med Imaging* 2004; 23: 137–152.
29. Fox MD, Snyder AZ, Vincent JL, et al. The human brain is intrinsically organized into dynamic, anticorrelated functional networks. *Proc Natl Acad Sci U S A* 2005; 102: 9673–9678.
30. Ryali S, Supekar K, Chen T, et al. Multivariate dynamical systems models for estimating causal interactions in fMRI. *Neuroimage* 2011; 54: 807–823.
31. Kelly AC, Di Martino A, Uddin LQ, et al. Development of anterior cingulate functional connectivity from late childhood to early adulthood. *Cereb Cortex* 2009; 19: 640–657.
32. van den Heuvel M, Mandl R, Luigjes J, et al. Microstructural organization of the cingulum tract and the level of default mode functional connectivity. *J Neurosci* 2008; 28: 10844–10851.
33. Hamilton JP, Chen G, Thomason ME, et al. Investigating neural primacy in major depressive disorder: multivariate Granger causality analysis of resting-state fMRI time-series data. *Mol Psychiatry* 2010; 16: 763–772.
34. May A. New insights into headache: an update on functional and structural imaging findings. *Nat Rev Neurol* 2009; 5: 199–209.
35. Menon V. Large-scale brain networks and psychopathology: a unifying triple network model. *Trends Cogn Sci* 2011; 15: 483–506.
36. Aderjan D, Stankewitz A and May A. Neuronal mechanisms during repetitive trigemino-nociceptive stimulation in migraine patients. *Pain* 2010; 151: 97–103.
37. Wiech K, Lin CS, Brodersen KH, et al. Anterior insula integrates information about salience into perceptual decisions about pain. *J Neurosci* 2010; 30: 16324–16331.
38. Coppola G, Di RA, Tinelli E, et al. Resting state connectivity between default mode network and insula encodes acute migraine headache. *Cephalalgia*. Epub ahead of print 1 January 2017. DOI: 10.1177/0333102417715230.
39. Li Z, Liu M, Lan L, et al. Altered periaqueductal gray resting state functional connectivity in migraine and the modulation effect of treatment. *Sci Rep* 2016; 6: 20298.
40. Roebroeck A, Formisano E and Goebel R. Mapping directed influence over the brain using Granger causality and fMRI. *Neuroimage* 2005; 25: 230–242.
41. Hwang K, Velanova K and Luna B. Strengthening of top-down frontal cognitive control networks underlying the development of inhibitory control: a functional magnetic resonance imaging effective connectivity study. *J Neurosci* 2010; 30: 15535–15545.
42. Luo Q, Ge T, Grabenhorst F, et al. Attention-dependent modulation of cortical taste circuits revealed by granger causality with signal-dependent noise. *PLoS Comput Biol* 2013; 9: e1003265.
43. Seth AK, Chorley P and Barnett LC. Granger causality analysis of fMRI BOLD signals is invariant to hemodynamic convolution but not downsampling. *Neuroimage* 2013; 65: 540–555.